SCIENCE ADVANCES | RESEARCH ARTICLE

CHEMICAL PHYSICS

# A spongy nickel-organic $CO_2$ reduction photocatalyst for nearly 100% selective CO production

Kaiyang Niu,[1,2]* You Xu,[3,4]* Haicheng Wang,[2,5]* Rong Ye,[2,6] Huolin L. Xin,[7] Feng Lin,[8] Chixia Tian,[9] Yanwei Lum,[1,2] Karen C. Bustillo,[10] Marca M. Doeff,[9] Marc T. M. Koper,[11] Joel Ager,[1,2] Rong Xu,[3,4]† Haimei Zheng[1,2]†

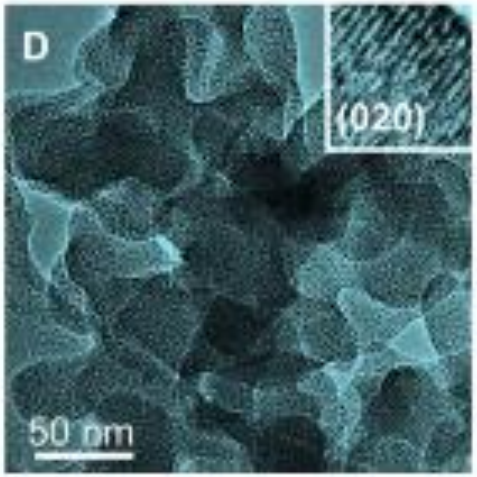


*Science Advances*
*Volume 3(7):e1700921*
*July 28, 2017*

Sandeep Bose
27-1-18

# Introduction

- Rapid fossil fuel consumption induces environmental burden and energy crisis.

- Excessive anthropogenic $CO_2$ emission is a significant concern because of its hastening impact on climate change, acidification of ocean, crop yield reduction, extinction of animal species, and damage to human health.

- Removal of excessive $CO_2$ from the atmosphere, particularly converting $CO_2$ to fuels using solar energy, is currently a global research endeavor. Discovering novel catalysts that can reduce the stable $CO_2$ molecules and convert them to liquid fuels with high activity and selectivity is essential.

- To date, despite the progress that has been made in investigating the photocatalytic reduction of $CO_2$, controlling the reaction to yield a specific product among many possible reaction species, including CO, $H_2$, $CH_4$ and formic acid remains a great challenge.

# In this paper

Developed photocatalysts that can efficiently convert $CO_2$ to CO and largely suppress other competing photocatalytic reactions, such as $H_2$ evolution, which is a critical step forward toward practical solar-to-fuels conversion for the production of high-value multicarbon fuels.

# Synthesis

TEG solutions (1 ml) of 1.5 M transition metal nitrates were added into 5 ml of DMF solution of 0.5 M TPA; the mixed solutions were stirred for 30 min before laser irradiation.

Typically, 3-hour laser irradiation was required for a 6-ml mixed precursor solution to complete the reaction.

Precipitates produced after laser irradiations or heating were rinsed with acetone/ethanol, centrifuged at 9000 rpm for three times, and then dried in air at 60°C to obtain powders.

3 mg of catalyst (for each test), 2.5 mmol of $Ru(bpy)_3Cl_2 \cdot 6H_2O$, and 2 ml of TEOA were added to10 ml of acetonitrile/$H_2O$ solvent mixture ($CH_3CN/H_2O$ = 8:2).

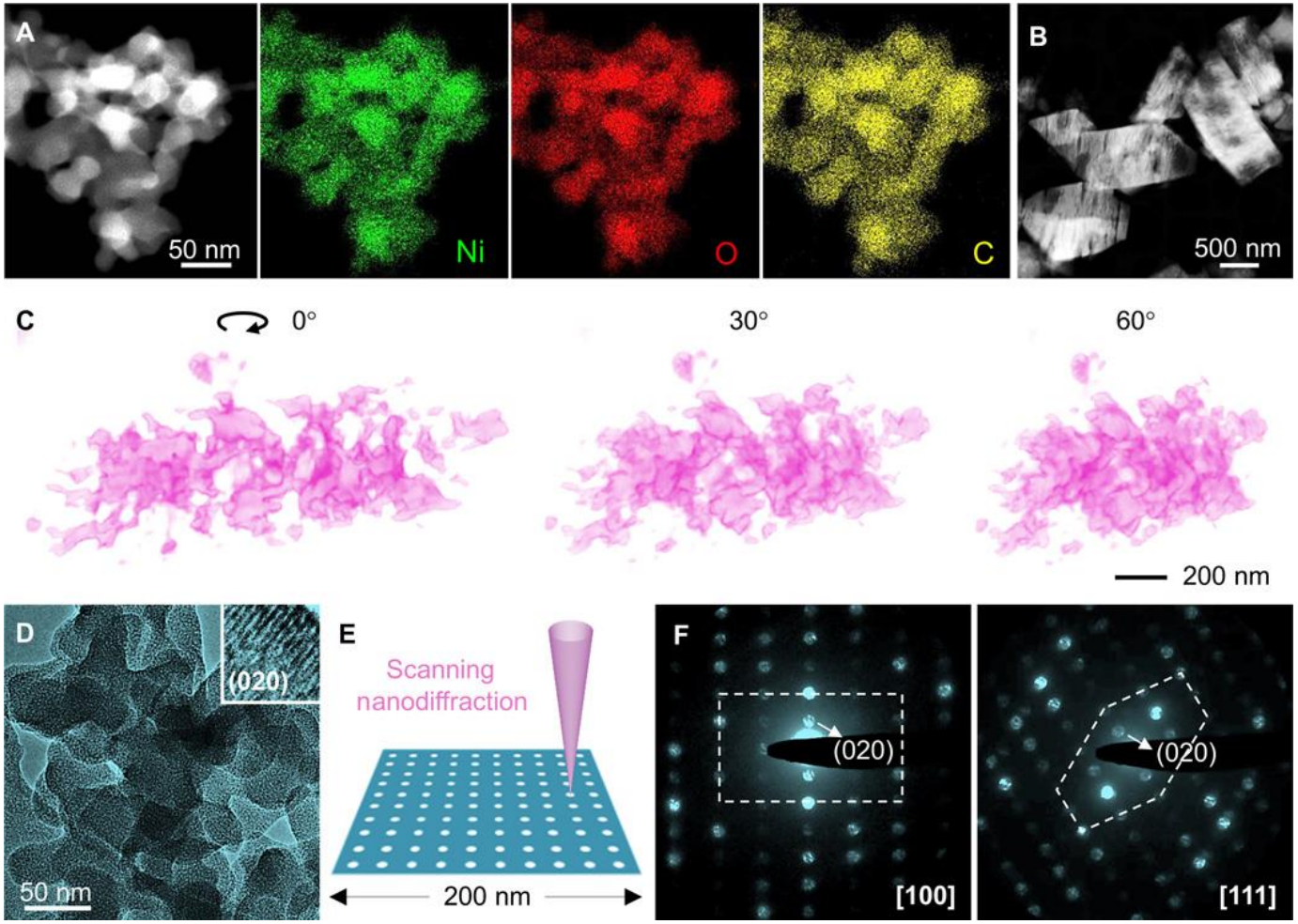


Fig. 1. Structure of the laser-chemical tailored spongy Ni(TPA/TEG) catalyst. (A) Scanning TEM (STEM) images and energy-dispersive x-ray spectroscopy (EDX)mapping of the spongy Ni(TPA/TEG) nanostructure. (B) STEM image of the Ni(TPA/TEG) particles. (C) Three-dimensional tomographic reconstruction of a fraction of spongy Ni(TPA/TEG) composite. (D) TEM image of the spongy Ni(TPA/TEG) nanostructure. The inset high-resolution TEM image displays the defective (020) lattices [d(020) =1.02 nm] of an orthorhombic crystal. (E) Scanning electron nanodiffraction series taken from the Ni(TPA/TEG) particle by a scanning nanoprobe with an electron beam size of ~3 nm.(F) Diffraction patterns showing the [100] and [111] orientations of the orthorhombic Ni(TPA/TEG) composite. The dimensions of the diffraction patterns are 11.9 nm-1 × 11.9 nm-1.

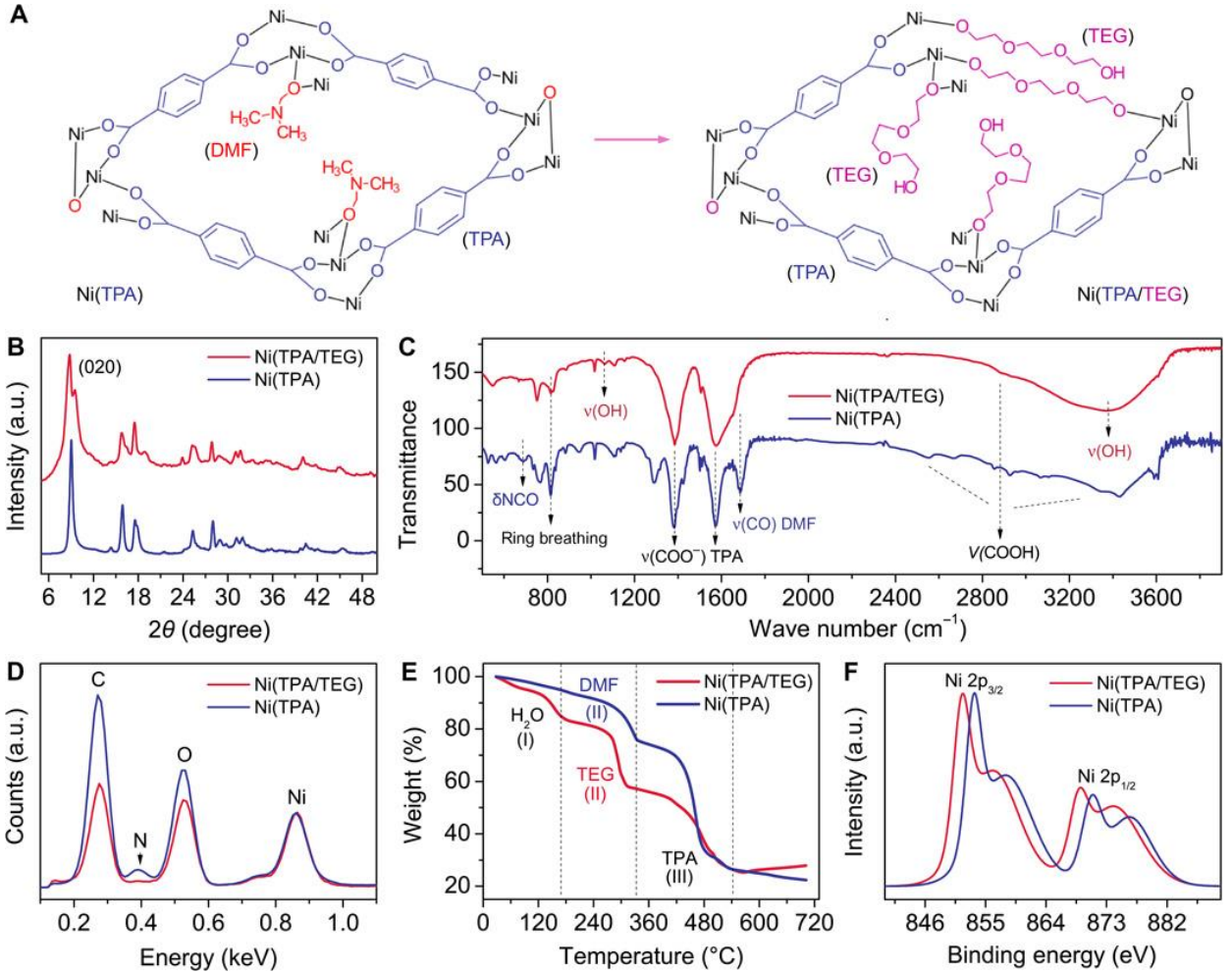


Fig. 2. Comparison of laser-chemical tailored Ni(TPA/TEG) and Ni(TPA) composites. (A) Proposed design strategy of the disordered spongy Ni(TPA/TEG) composite by introducing soft Ni-TEG building units into a Ni(TPA) framework through laser-chemical reaction. XRD patterns (B), FTIR spectra (C), EDX spectra (D), TGA curves (E), and XPS spectra (F) of the laser-chemical tailored Ni(TPA/TEG) and Ni(TPA) composites. a.u., arbitrary units.

When the TEG molecules, which lack essential carboxylic groups for the perfect framework construction, are weaved into the metal-TPA framework, their substitution of TPA linkers may frustrate the growth of highly ordered MOF crystals, resulting in disordered and defective metal-organic hybrids for effective CO2 fixation.

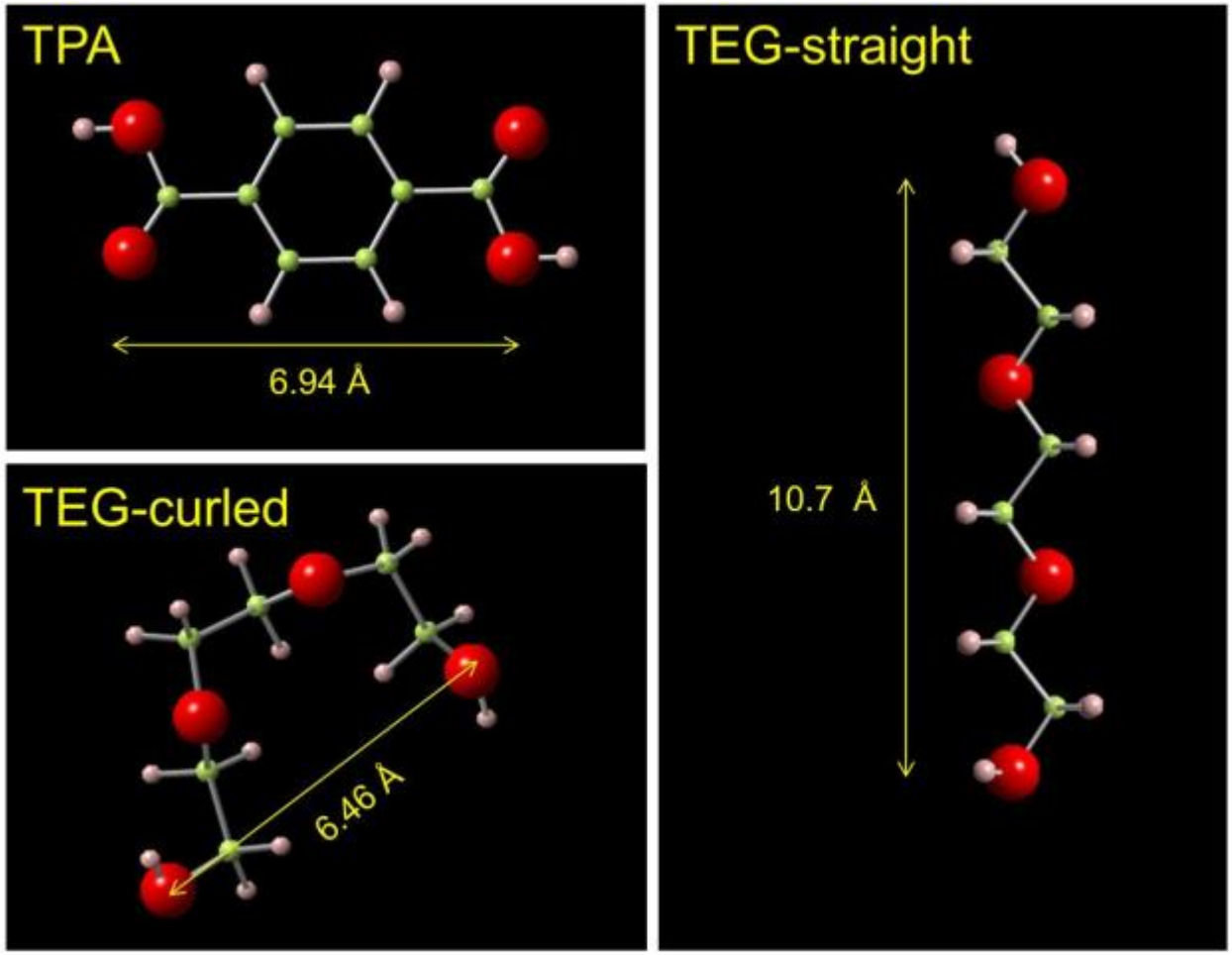


When the TEG molecules, which lack essential carboxylic groups for the perfect framework construction, are weaved into the metal-TPA framework, their substitution of TPA linkers may frustrate the growth of highly ordered MOF crystals, resulting in disordered and defective metal-organic hybrids for effective CO2 fixation.

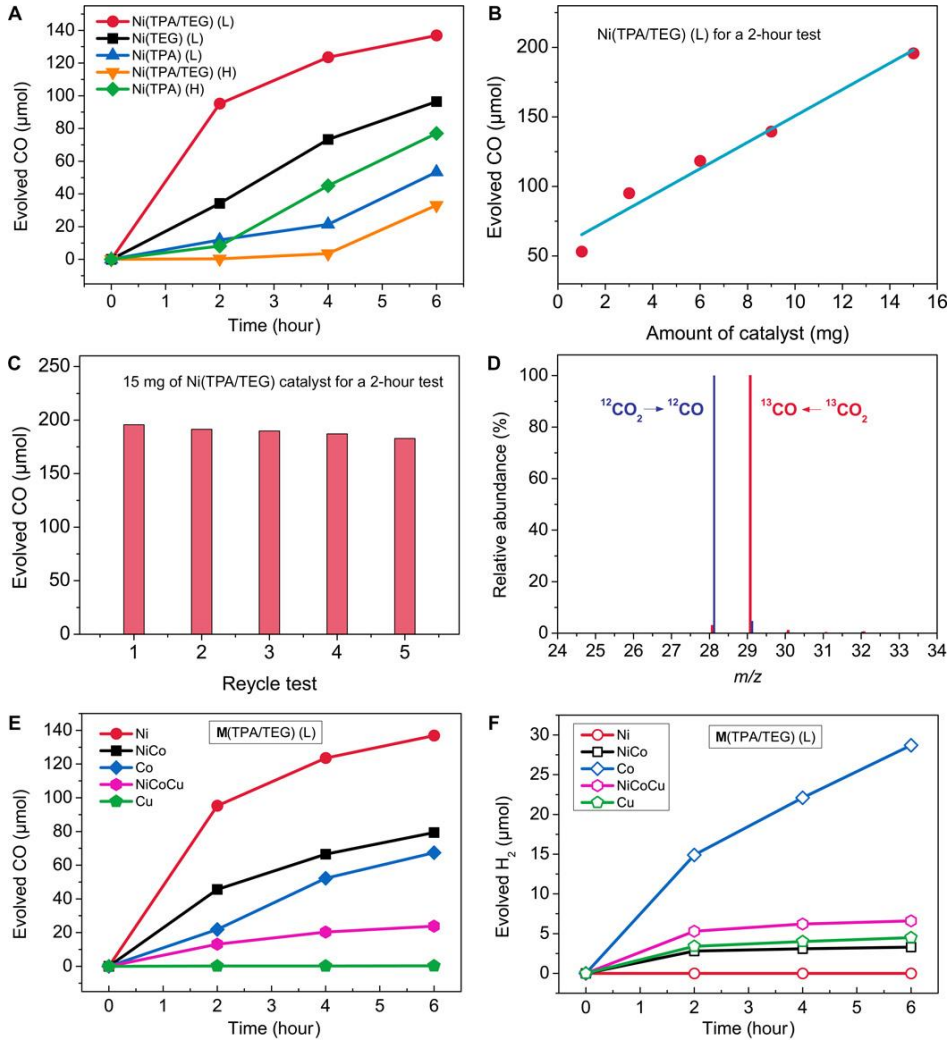


Fig. 3. Conversion of CO2 to CO by photocatalysis. (A) CO evolution on five Ni-based catalysts with different combinations of TPA, TEG, and DMF. The composites synthesized by laser-chemical approach are labeled with "L"; the ones synthesized by traditional heating method are marked with "H." (B) CO production on different amounts of the Ni(TPA/TEG) catalyst. (C) Average yield of CO in the first 2 hours for five recycling tests. (D) MS of 12CO (blue lines) and 13CO (red lines) produced on the spongy Ni(TPA/TEG) catalyst by using 12CO2 and 13CO2 as gas sources, respectively. m/z, mass/charge ratio. (E) Comparison of CO evolution on five laser-synthesized M(TPA/TEG) (M = Ni, Co, Cu) catalysts. (F) Comparison of H2 evolution on the five M(TPA/TEG) catalysts.

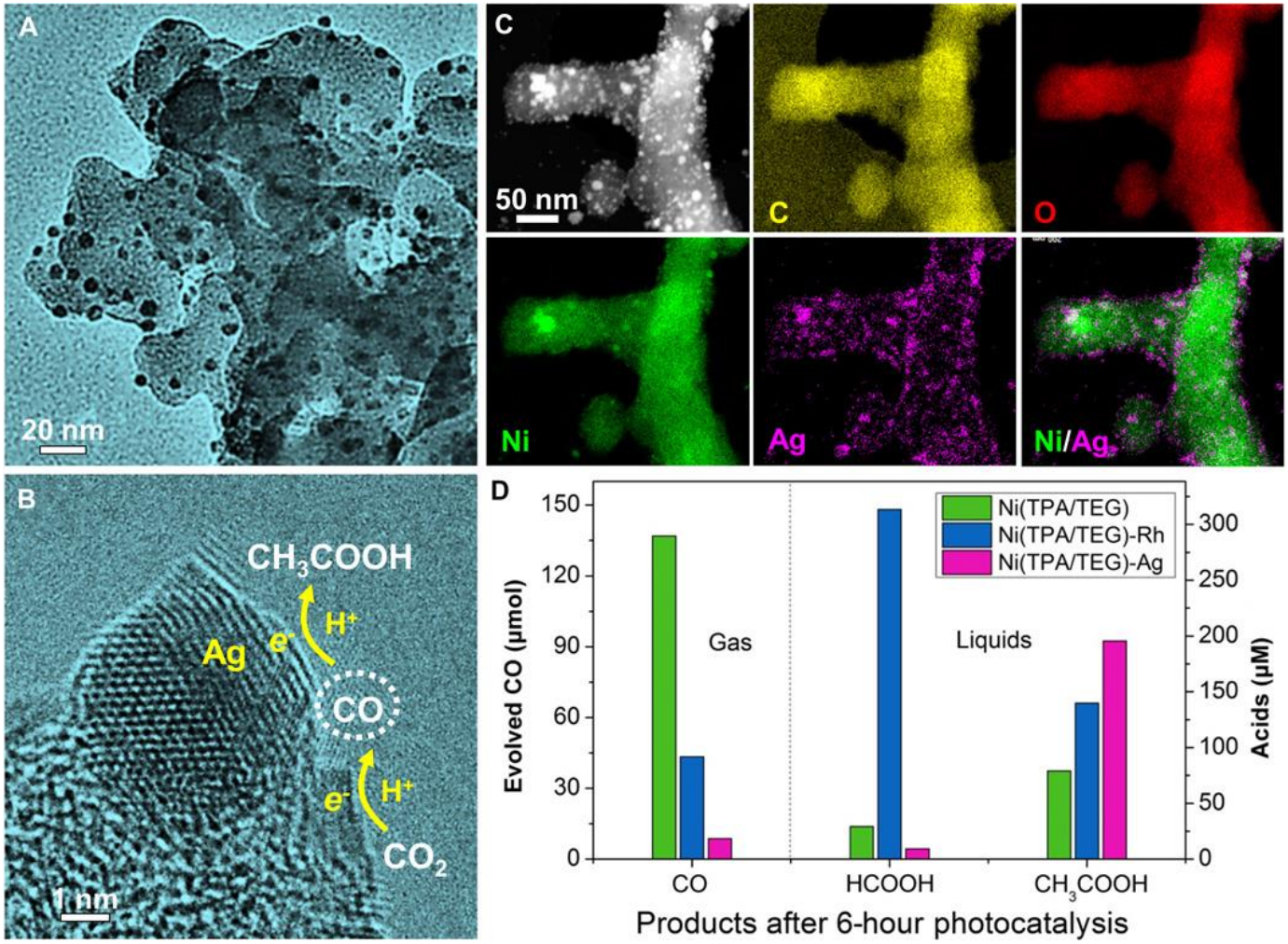


Fig. 4. Generation of liquid products on metal-decorated Ni(TPA/TEG) composites. Low-magnification (A) and high-resolution (B) TEM images of the Ni(TPA/TEG) composite decorated with Ag nanocrystals. (C) EDX mapping of the as-prepared Ni(TPA/TEG)-Ag composite. (D) Comparison of the amount of the products (CO, HOOH, and CH3COOH) generated from photocatalytic CO2 reduction on Ni(TPA/TEG), Ni(TPA/TEG)-Rh, and Ni(TPA/TEG)-Ag catalysts.

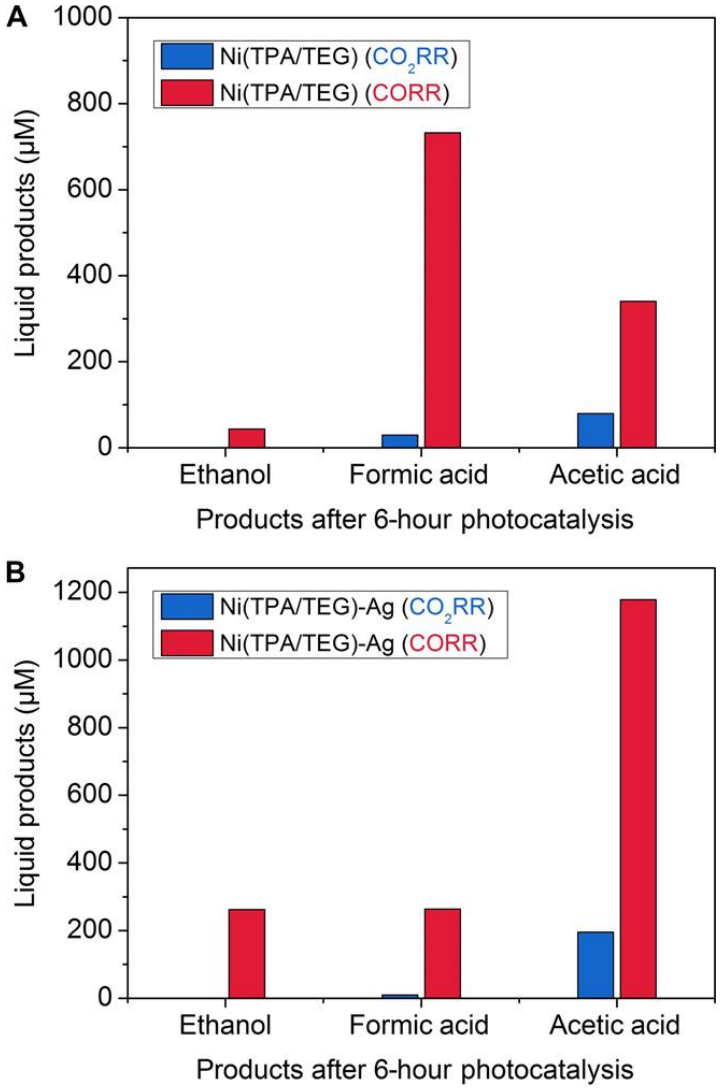


Fig. 5. Comparison of the liquid products generated from photocatalytic CO2 reduction reactions (CO2RR) and CO reduction reactions (CORR) on two catalysts. (A) Ni(TPA/TEG). (B) Ni(TPA/TEG)-Ag.

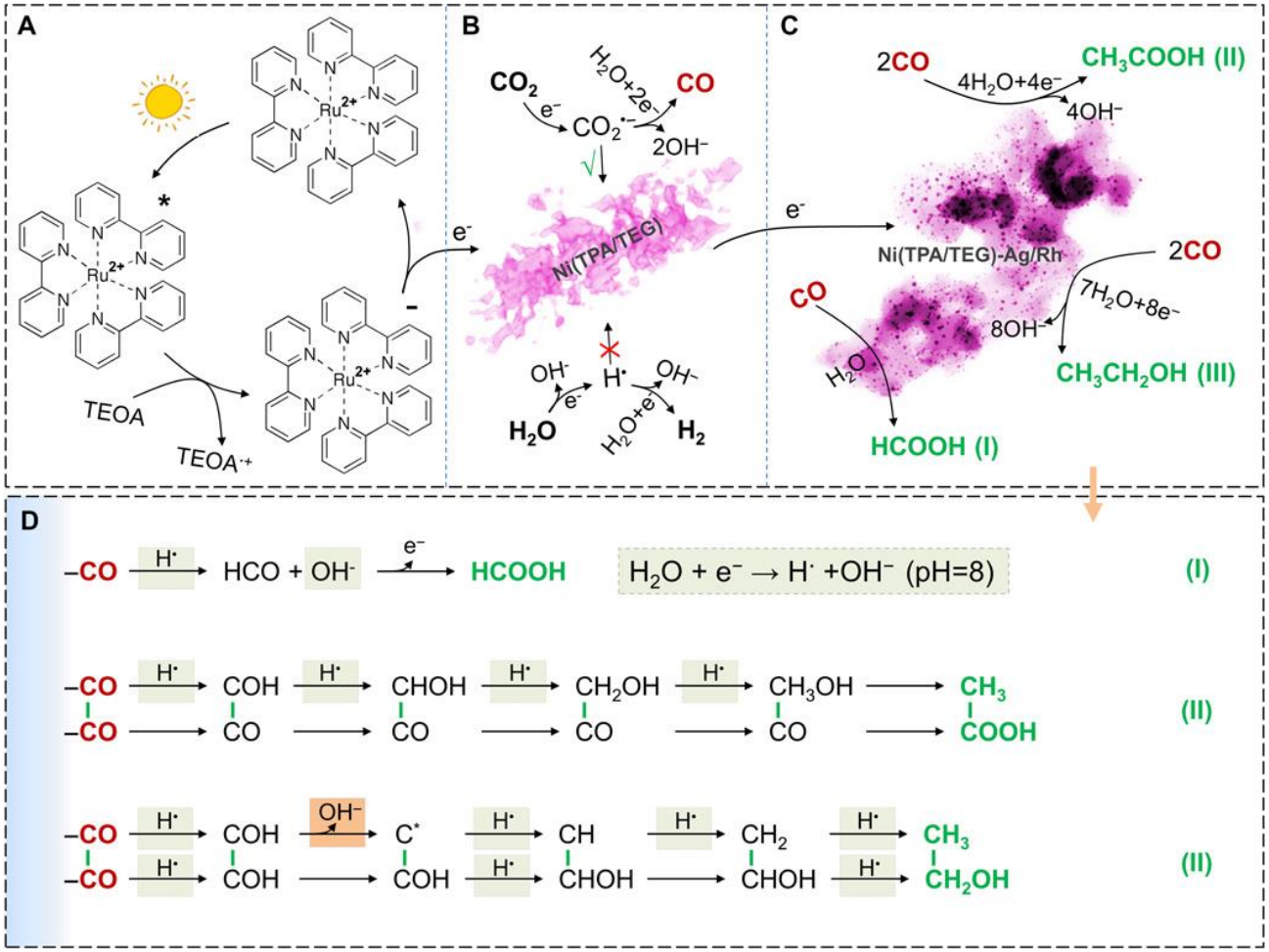


Fig. 6. Proposed mechanisms for the photocatalytic conversion of CO2 to CO and of CO to other liquid products.
(A) Visible light reduction of the photosensitizer [Ru(bpy)3]2+, which transfers an electron to the Ni(TPA/TEG) catalyst
(B) to convert CO2 to CO (B) and to Ni(TPA/TEG)-(Ag/Rh) catalysts for the generation of HCOOH, CH3COOH, and CH3CH2OH fromfurther reduction of CO (C). The STEM image in (C) is the Ag-decorated Ni(TPA/TEG) catalyst
(D) Possible conversion pathways leading to the formation of HCOOH, CH3COOH, and CH3CH2OH via proton-coupled one-, four-, and eight-electron steps, respectively.

# Summary

In summary, they have demonstrated a photochemical strategy for the design of novel nanostructured metal-organic materials, where the rigid TPA and soft TEG molecules are successfully cross-linked together with the Ni2+ centers.

A spongy Ni(TPA/TEG) hybrid structure with a considerably high concentration of defects is remarkably active for CO production (with a production rate of 15,866 mmol hour $g^{-1}$) from the heterogeneous photocatalytic CO2 reduction reaction, during which no other measurable competing gases such as H2 or CH4 are generated, thus giving a near 100% CO selectivity over other gases.

When the spongy Ni-organic catalyst is enriched with Rh or Ag nanocrystals, formic acid and acetic acid can be produced selectively from the photocatalytic CO2 reduction reactions.

More advanced metalorganic heterogeneous photocatalysts with improved CO2 fixation and light-harvesting capabilities are expected to be fabricated using the photochemical strategy for efficient solar to fuel conversion.


Thank
You